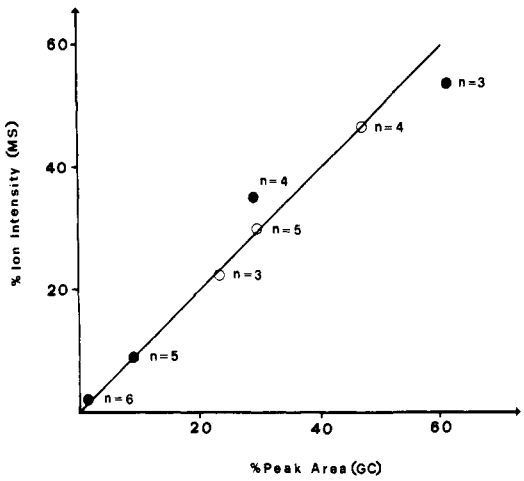

Figure 5. Percent ion intensity (MS) vs. percent peak area (GC) for each cyclic dimethylsiloxane present in two mixtures (○): n = 3 (24%), n = 4 (48%), n = 5 (28%); (●): n = 3 (62%), n = 4 (28%), n = 5 (9%), n = 6 (1%).

It is interesting to note that the product distribution obtained by DP–MS is similar to that observed in flash pyrolysis[14] and TGA[13] experiments.

Acknowledgment. Financial support from the Italian Ministry of Public Education is gratefully acknowledged.

Registry No. NaOH, 1310-73-2.

References and Notes

(1) S. Foti and G. Montaudo, in "Analysis of Polymer Systems", L. S. Bark and N. S. Allen, Eds., Applied Science Publishers, London, 1982, p 103.
(2) R. Adams, *J. Polym. Sci., Polym. Chem. Ed.*, **20**, 119 (1982).
(3) R. M. Lum, *J. Polym. Sci., Polym. Chem. Ed.*, **17**, 206 (1979).
(4) Y. Shimizu and B. Munson, *J. Polym. Sci., Polym. Chem. Ed.*, 17, 1991 (1979).
(5) R. D. Sedgwick, in "Developments in Polymer Characterization, Part 1", J. D. Dawkins, Ed., Applied Science Publishers, London, 1978, p 217.
(6) G. Montaudo, M. Przybylski, and H. Ringsdorf, *Makromol. Chem.*, **176**, 1753, 1763 (1975).
(7) A. Ballistreri, S. Foti, P. Maravigna, G. Montaudo, and E. Scamporrino, *J. Polym. Sci., Polym. Chem. Ed.*, **18**, 1923 (1980); **19**, 1679 (1981); **20**, 1685 (1982).
(8) S. Foti, A. Liguori, P. Maravigna, and G. Montaudo, *Anal. Chem.*, **54**, 674 (1982).
(9) S. Foti, P. Maravigna, and G. Montaudo, *Macromolecules*, **15**, 883 (1982).
(10) J. A. Semlyen, *Adv. Polym. Sci.*, **21**, 41 (1976).
(11) T. H. Thomas and T. C. Kendrick, *J. Polym. Sci., Part A-2*, 7, 537 (1969).
(12) J. B. Carmichael and J. B. Kissinger, *Can. J. Chem.*, **42**, 1996 (1964).
(13) T. Howard Thomas and T. C. Kendrick, *J. Polym. Sci., Part A-2*, 7, 537 (1969).
(14) J. C. Kleinert and C. J. Weschler, *Anal. Chem.*, **52**, 1245 (1980).
(15) H. Zahn and G. B. Gleitsman, *Angew. Chem., Int. Ed. Engl.*, **2**, 410 (1963).
(16) E. J. Goethals, *Adv. Polym. Sci.*, **23**, 103 (1977).
(17) M. J. Hunter, J. F. Hyde, E. L. Warrick, and H. J. Fletcher, *J. Am. Chem. Soc.*, **68**, 667 (1946).
(18) S. R. Heller and G. W. A. Milne, EPA/NIH Mass Spectral Data Base, 1978.

Thermal Degradation of the Blend Poly(2,6-dimethyl-1,4-phenylene oxide)–Polystyrene

Janusz Jachowicz,* Marian Kryszewski, and Maria Mucha

Polymer Institute, Technical University, Lodz 90-542, Poland. *Received July 6, 1983*

ABSTRACT: Thermal decomposition of blends of poly(2,6-dimethyl-1,4-phenylene oxide) (PPO) with polystyrene (PS) and graft copolymers of PS with PPO under vacuum or in an inert atmosphere in the temperature range 320–380 °C has been examined. The overall character of the process has been investigated by using nonisothermal techniques such as thermogravimetric analysis and thermal volatilization analysis. It has been shown that polystyrene is stabilized in the presence of PPO and that the temperature of the maximum rate of PS decomposition is shifted toward higher temperatures. More precise analysis of the composition of degradation products and the shape of isothermal thermogravimetric curves indicate the following elementary steps of PS decomposition in the presence of PPO: initiation by random scission, propagation by unzipping and intramolecular chain transfer, and first-order termination. Phase structure of the blend and the abundance of labile PPO protons eliminate the process of intermolecular chain transfer. It has also been shown that the presence of PPO interferes with the process of intramolecular hydrogen transfer.

1. Introduction

Thermal decomposition of a polymer blend is not, in general, the superposition of the processes of degradation of its pure components. Several publications have been devoted to studies of the interactions between degrading components of polymer blends, for example, for the following systems: poly(methyl methacrylate)–poly(vinyl chloride),[1] polystyrene–poly(vinyl chloride),[2] polystyrene–poly(α-methylstyrene),[3] and polystyrene–poly(ethylene glycol).[4] Blends of poly(2,6-dimethyl-1,4-phenylene oxide) with polystyrene are of particular intrest due to their complete homogeneity[5] and broad commercial use. Thermal degradation of this system has not been examined so far. The aim of this paper is to investigate the observed stabilization effect of polystyrene in mixtures with PPO during thermal degradation.

2. Experimental Section

2.1. Materials. The two samples of polystyrene used throughout this work were prepared in a free radical polymerization (sample 1: M_v = 172 000, M_n = 100 000, M_v/M_n = 1.72; sample 2: M_v = 840 000, M_n = 450 000, M_v/M_n = 1.87). M_v molecular weights were determined by the use of a viscosimetric method in toluene (25 °C, $K = 1.16 \times 10^{-4}$, $a = 0.72$[6]). M_n molecular weights were determined by membrane osmometry. The molecular weight distribution of these samples is, thus, intermediate between "the most probable" and that resulting from termination by recombination.

* Present address: Clairol, Inc., Stamford, CT 06922.

0024-9297/84/2217-1315$01.50/0

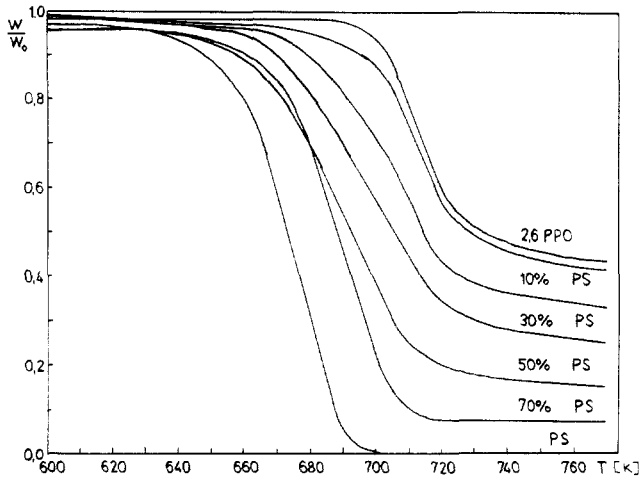

Figure 1. Nonisothermal thermogravimetric curves (heating rate 10 °C/min) of PS, PPO, and PPO–PS blends.

PPO was obtained from the Institute of Industrial Chemistry (Warsaw, Poland) and had been prepared by oxidative polycondensation of 2,6-xylenol (M_w = 41 500, M_n = 20 000). Prior to use the polymer was purified by three reprecipitations from benzene solution by methanol and dried overnight at 60 °C under vacuum.

Description of the samples of graft copolymers of PS with PPO is in the paper on the phase structure of the system PPO–PS.[5]

Foils of the blends were prepared by casting on a hot plate PPO–PS solutions of appropriate composition in toluene. For pure PPO, the temperature of the plate cannot be lower than 80 °C, for at lower temperatures, PPO crystallizes. In the case of the blends, the temperature of film casting can be lower (60–80 °C). Degradation studies were performed on thin films of thickness 15–20 μm. The films were extracted with methanol in order to remove residual solvent and dried for a few days at 60 °C under vacuum.

2.2. Thermal Decomposition. Nonisothermal degradation of the blends and copolymers was investigated by thermogravimetric analysis (TGA) using a Perkin-Elmer thermobalance TGS-1 in a nitrogen atmosphere in the temperature range 25–500 °C. The weight of the samples was 4 mg and the rate of heating 8 °C/min. Isothermal rates of volatilization were determined by using 20-mg samples in a vacuum (10^{-2} mmHg) and a thermobalance similar to that described by Madorsky.[7] Temperatures were in the range 300–360 °C. For molecular weight measurements of the residues, 400-mg samples were pyrolyzed under vacuum at 368 °C. The time scale of the experiment, depending upon the temperature of degradation, ran from 1 to 5 h. In the region 0–15% conversion the temperature was not constant, since the sample was being heated from room temperature to the temperature of the experiment, so experimental points taken within this region of conversions were not taken into consideration.

In order to obtain degradation products for gas chromatographic and mass spectroscopic analysis, 100-mg homopolymer and blend samples were degraded under vacuum (10^{-3} mmHg) in sealed tubes. Volatile degradation products trapped out at liquid nitrogen temperature as well as the cold ring fraction were washed out with a solvent (methylene chloride or benzene). The solution of the degradation products was subsequently subjected to mass spectroscopic analysis and gas chromatographic separations.

2.3. Analytical Techniques. Gas–liquid chromatography analysis was carried out with a GCHF 18.7 gas chromatograph equipped with a flame ionization detector. For all separations, 2-m columns packed with 5% SE-30 or 10% OV-101 coated on glass beads were used. Programed heating was used from 30 to 250 °C at a heating rate of 8 °C/min.

Mass spectrometry and gas chromatrography–mass spectrometry analysis was carried out with a 2091 LKB gas chromatograph/mass spectrometer connected to PDP 11 digital computer.

3. Results and Discussion

3.1. Phase Structure of Blends and Graft Copolymers. The analysis of phase structure of the blends and graft copolymers on the basis of dilatometric measurements is given in our preceding paper.[5] It was found, in accordance with other literature data,[8] that physical mixtures of PPO–PS formed homogeneous systems over the whole composition range. In contrast to physical blends, graft copolymers of PS with PPO were determined to be two-phase systems.

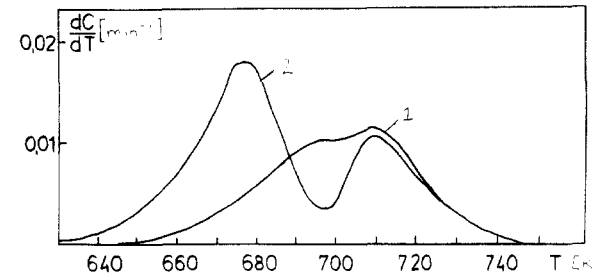

Figure 2. Differential thermogravimetric curves: (1) experimental curve for 60% PPO–40% PS; (2) theoretical curve for the same blend obtained from the superposition of the thermogravimetric curves of pure PPO and PS.

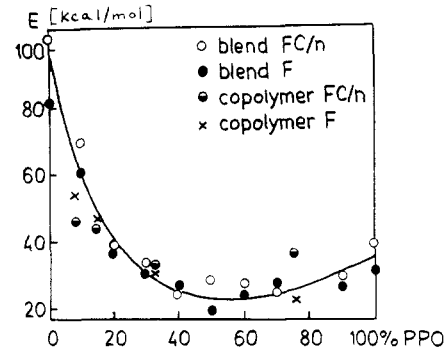

Figure 3. Activation energies of decomposition for the PPO–PS blends and copolymers calculated from nonisothermal thermogravimetric curves by the method of Freeman and Carrol (FC/n) and Fuoss (F) as a function of composition.

3.2. Nonisothermal Thermogravimetric Analysis. Integral thermogravimetric curves for the blends of different compositions are shown in Figure 1 (W_0 is the initial weight of the sample and W is the weight of the sample at conversion C). It may be concluded from Figure 1 that PPO is more stable than PS, and the TGA curves for the blends are situated between the curves obtained for pure PPO and PS. The addition of small amounts of PS to PPO decreases its stability only slightly, while the same amount of PPO added to PS causes an important increase of stability of this polymer. The effect of PS stabilization by PPO can be better illustrated by plotting differential thermogravimetric curves (DTG). Figure 2 shows the comparison of the DTG curve obtained from simple superposition of the thermogravimetric curves of pure PPO and PS with that obtained experimentally for the sample 60% PPO–40% PS. The calculated curve shows two distinctly separated maxima while in the case of the experimental curve, the PS maximum is shifted toward higher temperatures and overlaps the PPO maximum. Further support for the nonlinear effect of PS stabilization by PPO results from the activation energy calculations according to the methods described by Fuoss[9] and Freeman and Carrol.[10] In Figure 3, calculated activation energies for the blends and copolymers are plotted against the blend and copolymer composition. It is evident from the data shown in Figure 3 that the physical structure of PPO–PS mixtures has no effect on the kinetics of their decomposition (no difference between blends and copolymers).

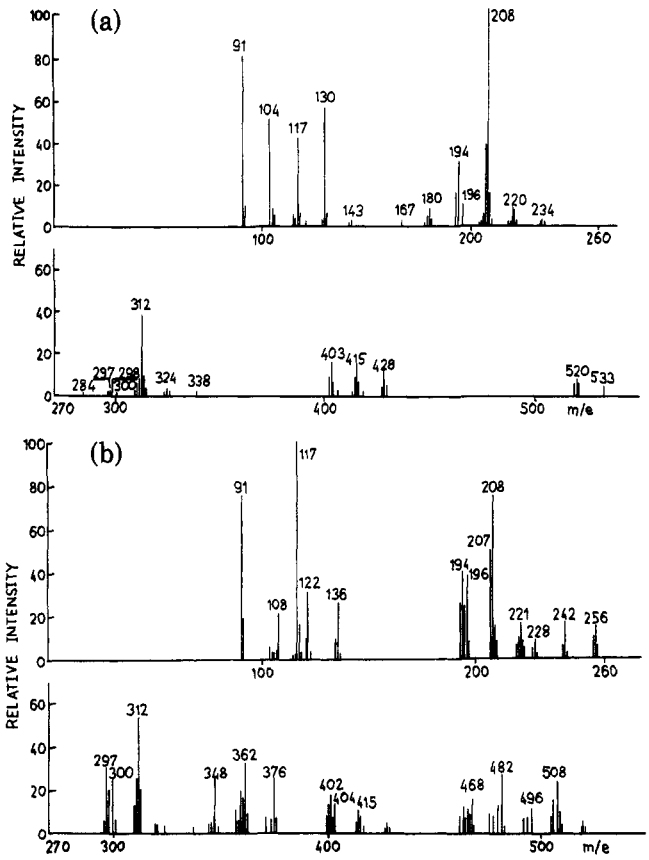

Figure 4. Mass spectra (15 eV) of the degradation products of (a) PS (b) 50% PS–50% PPO.

3.3. Degradation Products. The mass spectrum of the degradation products of PS, obtained by injecting the mixture of the degradation products directly into the ion source evaporator, is shown in Figure 4a. The presence of oligomeric species is a result of intramolecular proton transfer. On the basis of literature data,[7,11] it can be deduced that the general formula of the formed fragments are the following:

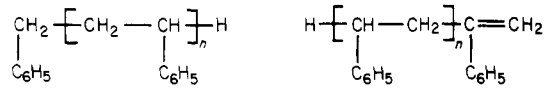

dimers: $n = 1$, M^+ 196, 208
trimers: $n = 2$, M^+ 300, 312
tetramers: $n = 3$, M^+ 404, 416
pentamers: $n = 4$, M^+ 508, 520
hexamers: $n = 5$, M^+ 612, 624

The above oligomers cannot be immediately seen in the mass spectra shown in Figure 4a as the molecular ions undergo strong fragmentation. To facilitate analysis of the mass spectrum shown in Figure 4a, the fragmentation patterns of the separated dimer (2,4-diphenyl-1-butene) and trimer (2,4,6-triphenyl-1-hexene) have to be taken into consideration (Chart I).

By comparing the mass spectrum of degradation products of PS in the mass range corresponding to dimeric products with the mass spectra of the dimer and trimer, one can observe that merely the ions at m/e 180, 196, and 220 (besides the ion at m/e 208) indicate the presence of appropriate dimers in the mixture. Dimer of molecular weight 220 was not detected in gas chromatography (Figure 5a). Molecular ions M^+ 196 and 208 form a dyad of dimeric products, while the compound of M^+ 182 was not identified (according to ref 11 it is diphenylethane). The region of the mass spectrum corresponding to trimeric products shows the presence of compounds of molecular

Chart I[a]

dimer (2,4-diphenyl-1-butene)

m/e 208 (100), molecular ion

m/e 130 (78), $CH_2{=}C(C_6H_5){-}CH{=}\overline{CH_2}]^{+\bullet}$

m/e 117 (24), $CH_2{=}C(C_6H_5){-}\overline{CH_2}]^{+}$

m/e 104 (54), $CH_2{=}\overline{CH}(C_6H_5)]^{+\bullet}$

trimer (2,4,6-triphenyl-1-hexene)

m/e 312 (13), molecular ion

m/e 221 (13), $CH_2{=}C(C_6H_5){-}CH_2{-}CH(C_6H_5){-}\overline{CH_2}]^{+}$

m/e 207 (100), $CH_2{=}C(C_6H_5){-}CH_2{-}\overline{C_7H_7}]^{+}$

m/e 194 (83), $HC{=}CH{-}\overline{CH_2}](C_6H_5)(C_6H_5)]^{+\bullet}$

m/e 117 (96), $CH_2{=}C(C_6H_5){-}\overline{CH_2}]^{+}$

[a] C_7H_7 = tropylium ion. The values given in parentheses are relative intensities.

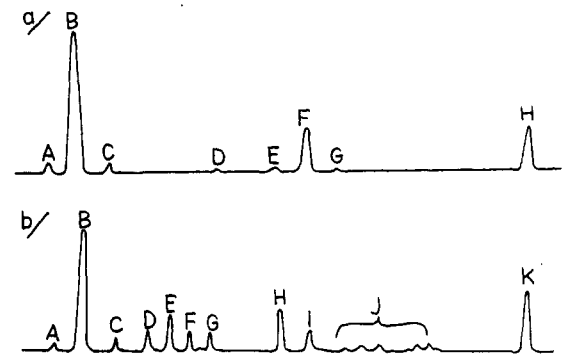

Figure 5. Gas chromatograms of degradation products. (a) PS: (A) ethylbenzene; (B) styrene; (C) α-methylstyrene; (D) product of molecular weight 182; (E) 1,3-diphenylpropane; (F) 2,4-diphenyl-1-butene; (G) product of molecular weight 208; (H) 2,4,6-triphenyl-1-hexene. (b) PS–PPO blend: (A) ethylbenzene; (B) styrene; (C) α-methylstyrene; (D) 2-methylphenol; (E) 2,6-dimethylphenol; (F) 2,4-dimethylphenol; (G) 2,4,6-trimethylphenol; (H) 1,3-diphenylpropane; (I) 2,4-diphenyl-1-butene; (J) dimers from PPO decomposition; (K) 2,4,6-triphenyl-1-hexene.

weights 300, 312, and 324. Trimer of molecular weight 312 was identified in gas chromatography (Figure 5a). Molecular ions M^+ 300 and 312 form a dyad of trimeric products. The dyads of higher molecular weight oligomers cannot be identified directly. It is plausible, as has been shown for alkylbenzenes, that the relative intensity of molecular ion in the mass spectra decreases with the increase of the chain length.[12] The scheme of fragmentation of higher oligomers is similar to the schemes suggested for 2,4-diphenyl-1-butene and 2,4,6-triphenyl-1-hexene. Analogously to the formation of the ions m/e 194, 207, and 221 from the trimer, its higher molecular weight analogues are formed: m/e 298, 402, and 504, m/e 311, 415, and 519

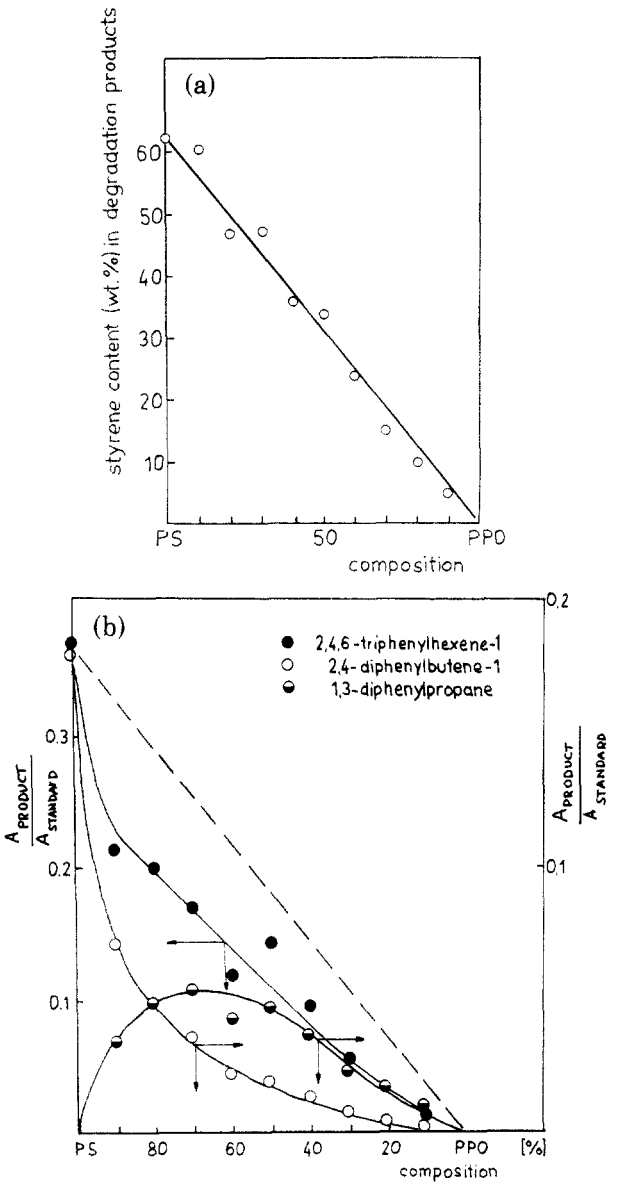

Figure 6. Yields of formation of (a) PS monomer and (b) PS dimer and trimer during degradation of the PS–PPO blends as a function of the blend composition.

and m/e 325, 429, and 533, respectively. These ions also appear in the mass spectrum (Figure 4a). Some of the compounds identified in the mass spectrum of degree of polymerization lower than 3 were detected in gas chromatograms (Figure 5a).

The gas chromatogram of the products from the degradation of the mixture 60% PPO–40% PS is shown in Figure 5b. A strong increase of the yield of 1,3-diphenylpropane and simultaneous decrease of the yield of 2,4-diphenyl-1-butene can be noted in comparison with the composition of degradation products of pure PS. Compounds D, E, F, G, and J are monomeric and dimeric degradation products of PPO. The analysis of gas chromatograms of degradation products of blends with higher PPO content has shown that the composition of the products characteristic for PPO is the same as for pure PPO.[13]

The same conclusions can be drawn from the analysis of the mass spectrum of degradation products of the blend 60% PS–40% PPO (degraded with a heating rate of 10 °C/min under vacuum). It shows an increase of the relative intensity of the ions m/e 196 and 300 (1,3-diphenylpropane and 1,3,5-triphenylpentane) (Figure 4b).

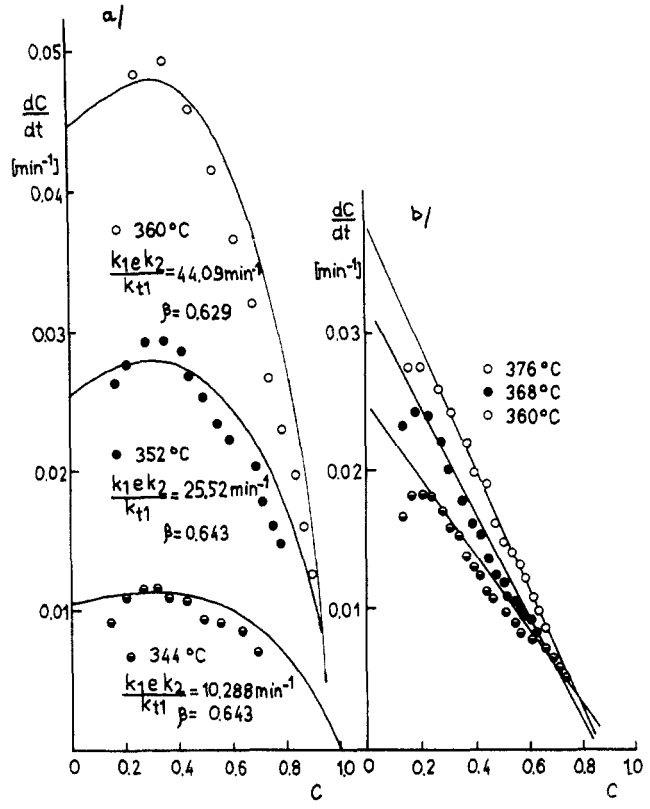

Figure 7. Isothermal differential thermogravimetric curves for PS (a) and PS degraded in the system 80% PS–20% PPO (b).

In the higher molecular mass region the molecular ions m/e 404 (1,3,5,7-tetraphenylheptane) and m/e 508 (1,3,5,7,9-pentaphenyloctane) are observed. The triads 108, 122, and 136 (monomers), 228, 242, and 256 (dimers), 348, 362, and 376 (trimers), and 468, 482, and 496 (tetramers) are characteristic for fragments formed in the thermal decomposition of PPO.[13]

Quantitative analysis of the yields of the main degradation products as a function of the blend composition was studied by means of gas chromatography. Styrene content was measured by using the calibration curve for styrene–cyclohexane. Results shown in Figure 6a indicate that the addition of PPO to PS, over the whole range of compositions, does not influence the depropagation process, as the experimental points describing the variation of styrene content in degradation products of the blends are placed along the straight line. On the other hand, PPO significantly influences the yields of intramolecular transfer products of PS (Figure 6b). Strong decrease of the yield of 2,4-diphenyl-1-butene is accompanied by the increase of the yield of 1,3-diphenylpropane. Decrease of the yield of 2,4,6-triphenyl-1-hexene is not so pronounced, which is probably due to more favorable steric conditions of trimer formation. The yields of formation of four main monomeric products of PPO decomposition (2-methylphenol, 2,6-dimethylphenol, 2,4-dimethylphenol, and 2,4,6-trimethylphenol) are slightly decreased (as compared with theoretical yields calculated by assuming the superposition of the compositions). This may result from such changes in morphological structure of the blend, as compared to pure PPO, which favors the formation of dimers and higher oligomers instead of monomers.

3.4. Isothermal Thermogravimetric Analysis. Isothermal thermogravimetric curves for pure PS and PS degraded in the blend with PPO are presented as the rate of volatilization, dC/dt, vs. conversion C, where

$$C = (W_0 - W)/W_0 \quad (1)$$

with W_0 the initial weight of the sample and W the weight of the sample at time t (Figure 7). The dC/dt were obtained by taking the slopes manually from the isothermal TG curves at various conversions (Figure 7a). The curves for PS degraded in the blend with PPO were obtained by subtracting the PPO part from the TG curve for the blend, assuming that the presence of PS does not modify the shape of the TG curve for PPO (Figure 7b). This assumption is supported by the results of nonisothermal thermogravimetric analysis, which shows that PPO modifies the curves of PS decomposition, while no effect of PS on decomposition of PPO was observed (Figure 2). Maximum rate of weight loss process for pure PS occurs at 32% conversion, which is in agreement with the earlier published results by Madorsky,[7] Wall,[14] and Jellinek.[15] Kinetic description of the decomposition process has been formulated by Simha,[16] Jellinek,[15] Boyd,[17] and Cameron.[18] It is generally agreed that the decomposition process is initiated at the chain ends, occurring in competition with random initiation (the ratio of the rate coefficients for random to end initiation has a value 3×10^{-4} at $C = 0$ for polymers prepared in radical polymerization[19]). It will be assumed in this discussion, for simplification, that initiation in pure PS is uniquely an end activating process. Intermolecular transfer and propagation by unzipping and intramolecular transfer are evident from earlier works.[3,14] Recently published results by Cameron and co-workers[20] show that termination is first order throughout the decomposition reaction, rather than second-order recombination. Taking into consideration these five elementary steps, similarly to Wall and co-workers,[19] the steady-state number of radicals is obtained from the following condition:

$$K_{t1}R(t) = K_{1e}Q(t) \tag{2}$$

$$R(t) = \frac{K_{1e}}{K_{t1}} \frac{V(t)}{P_n(t)} \frac{d_0}{m} \tag{3}$$

where K_{t1} is the rate coefficient for termination of radicals by a first-order process, K_{1e} is the rate coefficient for active radical formation at chain ends, $R(t)$ is the the sum of all radicals in the reacting system, $Q(t)$ is the the sum of all molecules in the reacting system, $P_n(t)$ is the number-average degree of polymerization at time t, $V(t)$ is the volume of the system from which volatiles are escaping, d_0 is the density of molten polymer, and m is the monomer molecular weight. On assumption that all weight loss arises from depropagation of macroradicals (by unzipping or intramolecular chain transfer) the rate of volatilization is obtained:

$$\frac{dC}{dt} = \frac{m}{W_0} \frac{dM}{dt} = \frac{m}{W_0} K_2 R(t) = \frac{K_{1e}K_2}{K_{t1}P_n(t)}(1 - C) \tag{4}$$

where K_2 is the rate coefficient for depropagation. The changes in degree of polymerization during degradation are caused by intermolecular chain transfer (lack of random scission):[17]

$$\frac{1}{P_n(t)^2} \frac{dP_n(t)}{dt} = -K_I\bar{R}(t) \tag{5}$$

$\bar{R}(t) = R(t)/V(t)$ is the stationary concentration of radicals and K_I is the rate coefficient for intermolecular chain transfer. From combination of eq 4 with eq 5 and integration, it follows that

$$\ln (1 - C) = -\frac{mK_2}{K_I d_0}\left(\frac{1}{P_n(t)} - \frac{1}{P_n(0)}\right) = -\beta\left(\frac{P_n(0)}{P_n(t)} - 1\right) \tag{6}$$

$$\beta = \frac{mK_2}{K_I d_0 P_n(0)}$$

The values of the parameters $(K_{1e}K_2)/K_{t1}$ and β for calculations of theoretical differential thermogravimetric curves fitting the experimental data were obtained from the following conditions:

$$1 - C_{max} = e^{-1+\beta} \tag{7}$$

$$\left(\frac{dC}{dt}\right)_{max} = \frac{K_{1e}K_2}{K_{t1}} \beta P_n(0)(1 - C_{max}) \tag{8}$$

where C_{max} is the conversion at which

$$dC/dt = \max = (dC/dt)_{max}$$

The best fit to experimental points was obtained for the values of β and $(K_{1e}K_2)/K_{t1}$ given in Figure 7a. The overall agreement with the experimental data is similar to that shown in the paper of Wall and co-workers.[19] The value of $(K_{1e}K_2)/K_{t1} = 25.5$ min^{-1} at 352 °C is in fair agreement with that (41.9 min^{-1} at 353 °C) mentioned by Cameron.[20]

Integral thermogravimetric curves shown in Figure 8 confirm the result described earlier in the literature that polystyrene of high molecular weight (M_n = 450 000) is more stable than lower molecular weight polystyrene (M_n = 100 000). Both polystyrene samples had similar polydispersity (M_w/M_n = 1.7). This justifies the assumption that thermal degradation of PS is initiated at the polymer chain ends. On the other hand, TG curves obtained for mixtures of PS (M_n = 450 000) with PPO (M_n = 22 000) (80% PS–20% PPO) and PS (M_n = 100 000) with PPO (M_n = 22 000) (of the same composition) indicate that both blends exhibit the same thermal stability. It means that the influence of molecular weight on thermal stability of PS disappears in mixtures with PPO.

All these experimental data allow one to conclude that stabilization of PS in blends with PPO is due to the change of the mechanism of PS decomposition. If we assume that a "cage effect" plays an important role in the initiation process (it explains why the initiation in pure PS takes place at the chain ends), then its influence on the effective bond scission should be limited in the case of the PS–PPO blends due to the high concentration of protons able to deactivate the macroradicals formed after scission. That is why it seems natural that the end activation (scission in the vicinity of polymer ends) transforms into statistical scission. Another argument that supports this suggestion is the observed decrease of intrinsic viscosity of the degraded sample as a function of conversion. If intermolecular transfer disappears in the blends, which seems reasonable because of the presence of labile PPO protons, then the decrease of molecular weight should be caused by random scission. Differential isothermal thermogravimetric curves for PS degraded in the blend with PPO have the maximum rate of weight loss at about 19% conversion. In comparison with the TG curves for pure PS, they are shifted toward lower conversions. This also seems to suggest the disappearance of intermolecular chain transfer.[17] In formulating the kinetic model of PS degradation in the presence of PPO, we must take note of the following features of this reaction: (1) degradation is initiated by random chain scission; (2) intermolecular chain transfer is not operative ($K_I = 0$); (3) depropagation takes place by unzipping and intramolecular chain transfer; (4)

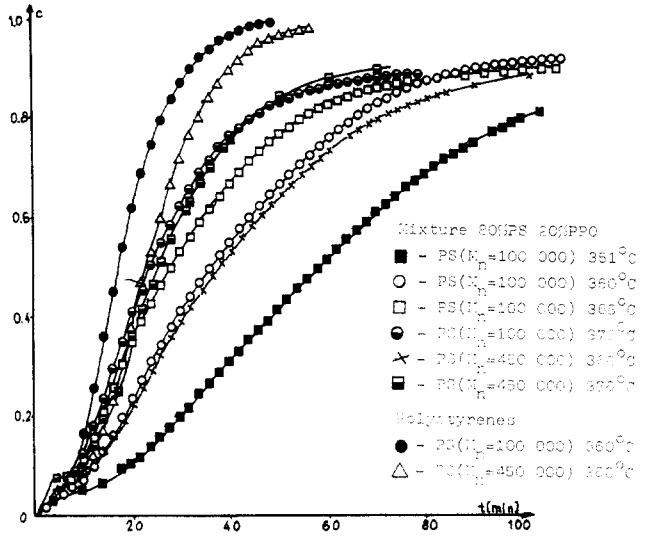

Figure 8. Integral isothermal thermogravimetric curves for the blends 80% PS–20% PPO (M_n(PPO) = 22 000).

Scheme I

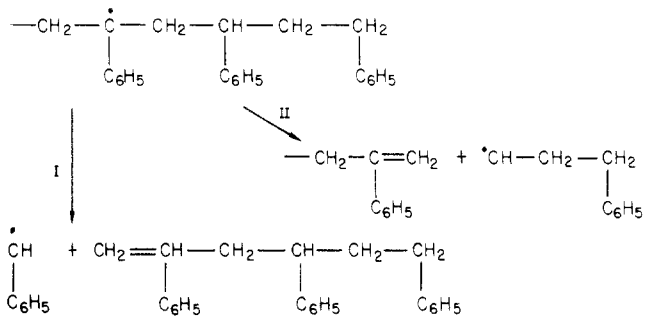

termination, due to the presence of PPO, is a first-order reaction. Introduction of these assumptions into the kinetic model leads to the following equations:

steady-state number of radicals

$$K_{t1}R(t) = 2K_{1s}Q(t)\bar{P}_n(t)$$

$$R(t) = (2K_{1s}V(t)d_0)/K_{t1}m \quad (9)$$

rate of volatilization

$$\frac{dC}{dt} = \frac{m}{W_0}K_2R(t) = \frac{2K_{1s}K_2}{K_{t1}}(1 - C) \quad (10)$$

where K_{1s} is the rate coefficient for random scission. Thus, the steady-state concentration of radicals and rate of volatilization are independent of molecular weight and the rate is a linear function of conversion. The maximum rate of reaction is at $C = 0$. These conclusions from the kinetic model are in fair agreement with experiment (Figure 7b). The slope of the straight line in Figure 7b yields a value 1.4×10^{-2} min^{-1} for $(K_{1s}K_2)/K_{t1}$ at 360 °C, which is in agreement with the value 6.0×10^{-3} min^{-1} at 353 °C obtained by Cameron and co-workers for degradation of pure PS.[20] Another possibility of PS stabilization is suggested by the results of the analysis of degradation products. The effect of increased yield of 1,3-diphenylpropane and its higher molecular weight analogues together with the decrease of the yield of 2,4-diphenyl-1-butene and 2,4,6-triphenyl-1-hexene provides, in our opinion, strong evidence for the significant role of a "cage effect" in the process of intramolecular proton transfer.

In Scheme I the product of 1,5 intramolecular chain transfer can decompose in two ways.[18] Reaction I is a form of propagation, for the depropagation center is reproduced together with the formation of mobile low molecular weight inactive product. Reaction II is a form of first-order termination, as it results in the formation of low molecular weight mobile radicals and a deactivated chain end. The reaction medium probably determines which of these reactions dominates during degradation. If the process is carried out in pure PS, reaction I prevails (high yield of alkenes) with a small contribution from reaction II (low yield of 1,3-diphenylpropane, Figure 6b). This is caused by a low probability of mobile radical termination. Alternatively, in the medium where labile protons able to deactivate radicals are abundant, reaction II predominates. In kinetic equations, depropagation by unzipping and intramolecular chain transfer is described by one complex rate coefficient of depropagation, K_2. The considered effect of the change of the mechanism of intramolecular chain transfer should manifest itself in the decrease of depropagation rate constant.

Conclusions

It seems that the most interesting feature of this work is that it reveals the important role of a cage effect in decomposition of polystyrene. This could be proven by the analysis of a weakly interacting system such as PPO–PS. The cage effect appeared to be decisive whether the initiation is a random scission process or whether the scissions are privileged at the ends of the chains. It also determines the course of intramolecular chain transfer which may be a form either of propagation or termination.

The foregoing analysis of the experimental data is compatible with the previous interpretations of the results of thermal decomposition of ultrathin PS films[21] and PS–poly(vinyl chloride) mixtures.[2] Observed stabilization effects of PS were thought to be caused by the physical structure of the sample, which significantly hinders or eliminates the reaction of intermolecular chain transfer. The results of the degradation of PS–PPO blend are also consistent with the data obtained for the blends PPO–poly(α-methylstyrene) and PPO–"head-to-head" polystyrene.[22] Neither poly(α-methylstyrene), which decomposes by "unzipping", or "head-to-head" polystyrene, which undergoes statistical scission, interacts with PPO during thermal degradation. We believe that this may be due to the lack of intermolecular chain-transfer processes in the mechanism of degradation of these two polystyrenes.

Acknowledgment. We thank M. Nawrocki for technical assistance in the gas chromatographic separations and preparation of the manuscript.

Supplementary Material Available: Mass spectra of the polystyrene dimer and trimer (2 pages). Ordering information is given on any current masthead page.

References and Notes

(1) I. C. McNeill and D. Neil, *Eur. Polym. J.*, **6**, 569 (1970); **6**, 143 (1970).
(2) B. Dodson and I. C. McNeill, *J. Polym. Sci., Polym. Chem. Ed.*, **14**, 353 (1976).
(3) D. H. Richards and D. A. Salter, *Polymer*, **8**, 127 (1967).
(4) L. P. Blanchard, V. Hornoff, H. Lam, and S. L. Malhotra, *Eur. Polym. J.*, **10**, 1057 (1974).
(5) M. Mucha, J. Jachowicz, and M. Kryszewski, *Acta Polym.*, **32** (3), 156 (1981).
(6) J. H. S. Green, *J. Polym. Sci.*, **34**, 514 (1959).
(7) S. L. Madorsky, "Thermal Degradation of Organic Polymers", Interscience, New York, 1964.
(8) E. O. Stejskal, J. Schaefer, M. D. Sefcik, and R. A. McKay, *Macromolecules*, **14**, 275 (1981); F. Mikes, H. Morawetz, and K. S. Dennis, *ibid.*, **13**, 969 (1980).
(9) R. M. Fuoss, I. O. Salyer, and H. Wilson, *J. Polym. Sci., Part A-1*, **2**, 3147 (1964).
(10) E. S. Freeman and B. Carrol, *J. Phys. Chem.*, **62**, 394 (1958).
(11) D. O. Hummel, H. J. Dussel, and K. Rubenacker, *Makromol. Chem.*, **145**, 267 (1971).

(12) H. Budzikiewicz, C. Djerassi, and D. H. Wiliams, "Mass Spectrometry of Organic Compounds", Holden-Day, San Francisco, Cambridge, London, and Amsterdam, 1967.
(13) J. Jachowicz, M. Kryszewski, and P. Kowalski, *J. Appl. Polym. Sci.*, **22**, 2891 (1978).
(14) L. A. Wall, S. Straus, J. H. Flynn, D. McIntyre, and R. Simha, *J. Phys. Chem.*, **70**, 53 (1966).
(15) H. H. G. Jellinek, "Thermal Degradation of Vinyl Polymers", Academic Press, New York, 1955.
(16) R. Simha, L. A. Wall, and P. J. Blatz, *J. Polym. Sci.*, **5**, 615 (1950); R. Simha and L. A. Wall, *ibid.*, **6**, 39 (1951).
(17) "Thermal Stability of Polymers", Vol. 2, R. T. Conley, Ed., Marcel Dekker, New York, 1970.
(18) G. G. Cameron, *Makromol. Chem.*, **100**, 255 (1967).
(19) L. A. Wall, S. Straus, R. E. Florin, and L. J. Fetters, *J. Res. Natl. Bur. Stand. (U.S.)*, **77A**, 157 (1973).
(20) G. G. Cameron, J. M. Meyer, and I. T. McWalter, *Macromolecules*, 11, 696 (1978).
(21) I. C. McNeill and M. A. J. Mohammad, *Eur. Polym. J.*, 8, 975 (1972).
(22) M. Kryszewski, J. Jachowicz, M. Malanga, and O. Vogl, *Polymer*, **23** (2), 271 (1982).

Photoluminescence Probes for the Investigation of Interactions between Sodium Dodecyl Sulfate and Water-Soluble Polymers

Nicholas J. Turro,* Bruce H. Baretz, and Ping-Lin Kuo

Department of Chemistry, Columbia University, New York, New York 10027.
Received January 18, 1983

ABSTRACT: Fluorescence probe techniques have been employed to monitor interactions between sodium dodecyl sulfate (SDS) and two water-soluble polymers, poly(*N*-vinylpyrrolidone) and poly(ethylene oxide). The results are analogous to those found by conventional methods and lead to the conclusion that SDS micelles bind to the polymers. The fluorescence probe method also provides information on the solubilization mechanism, since the site of solubilization of the probe can be inferred.

Introduction

Polymer/Surfactant Interactions in Aqueous Solution. Investigations of the interactions of polymers and surfactants in aqueous solution are of interest from the fundamental standpoint of obtaining an understanding of the structure and dynamics of polymer/surfactant associates and from the practical standpoint of employing fundamental understanding to assist in formulations for polymer/surfactant systems that can be used in the process of enhanced oil recovery.[1] The ability of surfactants to aggregate and form micelles[2] adds a particularly intriguing dimension to their interactions with polymers. An extensive body of evidence has accumulated that supports the proposal that anionic surfactants such as sodium dodecyl sulfate (SDS) and water-soluble polymers such as poly(*N*-vinylpyrrolidone) or poly(ethylene oxide) (PVP and PEO, respectively) form associates between surfactant aggregates and polymer rather than surfactant monomers and polymer.[3]

The following picture has emerged to describe the polymer/surfactant interactions that occur when SDS is added to a dilute aqueous solution of water-soluble PVP or PEO.[2-4] In the absence of polymer, SDS forms well-defined micelles above the critical micelle concentration (cmc) of 8×10^{-3} (termed x_0). When SDS is added to a dilute ($\lesssim 1\%$) solution of PVP (or PEO), there is no association between polymer and surfactant until a concentration x_1 is reached. Above x_1 (which is a lower concentration than the cmc, x_0) the polymer /surfactant association process starts abruptly and then saturates abruptly at a concentration x_2 (which is a higher concentration than the cmc, x_0). Thus, three well-defined regions are suggested by available information: region I, for which [SDS] ranges from 0 to x_1; region II, for which [SDS] ranges from x_1 to x_2; and region III, for which [SDS] is greater than x_2. In region I, there is no significant polymer/surfactant interaction. In region II, clusters of SDS molecules (termed premicelles) cooperatively associate with the polymers. In region III, free micelles of SDS form and exist in equilibrium with the polymer/surfactant associates. These situations are summarized schematically in Figure 1.

Pyrene and 11-(3-Hexyl-1-indolyl)undecyl Sulfate as Fluorescence Probes of Surfactant Association. Pyrene is a strongly hydrophobic probe with low solubility (ca. 3×10^{-7} M) in water. The fluorescence spectrum of pyrene at low concentration ($<1 \times 10^{-6}$ M) in homogeneous solutions possesses considerable fine structure whose relative peak intensities undergo significant perturbation upon going from polar to nonpolar solvents.[5] The ratio of the fluorescence intensity of the highest energy vibrational band (I_I) to the fluorescence intensity of the third highest energy vibrational band (I_{III}) has been shown to correlate with solvent polarity for a range of solvent structures. For example,[5] in hydrocarbon solvents I_I/I_{III} is ca. 0.6, in ethanol I_I/I_{III} is ca. 1.1, and in water I_I/I_{II} is ca. 1.6.

This distinct dependence of fluorescence vibrational fine structure has been utilized to investigate the formation of SDS micelles.[6] In the presence of SDS micelles, pyrene is preferentially solubilized in or near the interior hydrophobic region of the micelle. The value of I_I/I_{III} is ca. 1.1 when pyrene is solubilized in SDS micelles (Figure 2). Since the value of I_I/I_{III} for pyrene is a convenient, readily measured quantity and since pyrene is poorly water soluble and is preferentially solubilized in the hydrophobic regions of aqueous systems that are microheterogeneous, it seemed apparent that polymer/surfactant associations could be investigated by employing the I_I/I_{III} parameters.

The functionalized detergent 11-(3-hexyl-1-indoyl)undecyl sulfate (6-In-11$^-$) possesses a "built-in" fluorophore that allows this detergent to serve as a photoluminescence probe.[7] It has been shown that the fluorescence maximum (λ_F) of 6-In-11$^-$ is sensitive to solvent polarity so that λ_F (in a manner similar to I_I/I_{III}) may be employed to probe the formation of hydrophobic associates in aqueous solution.

Results

Pyrene as a Fluorescence Probe for Polymer/Surfactant Interactions for the PVP/SDS and PEO/SDS Systems. The variation of I_I/I_{III} was measured for aqueous solutions containing fixed concentrations of

0024-9297/84/2217-1321$01.50/0